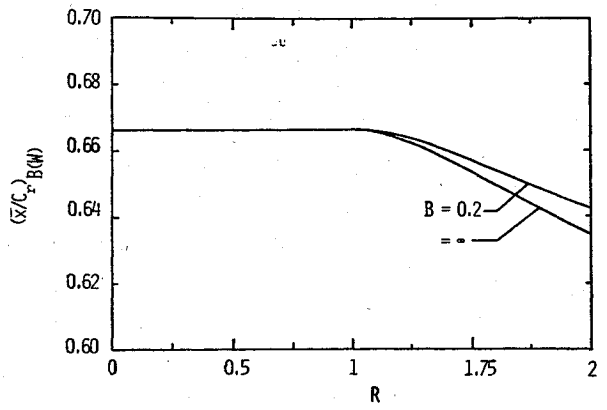

Fig. 3 $(\bar{x}/C_r)_{B(W)}$ **for negative afterbody as a function of** B **and** R.

Obviously $(\bar{x}/C_r)_{B(W)}(R \le 0) = 0$. Note that $(\bar{x}/C_r)_{B(W)}$ in the case of negative afterbody depends only on the parameters B and R. Variation of $(\bar{x}/C_r)_{B(W)}$ with respect to R and B is illustrated in Fig. 3. The dependence on B is again weak. It is interesting to note that when $0 \le R \le 1$, $(\bar{x}/C_r)_{B(W)} = \frac{2}{3}$, a constant. This indicates a proportional variation of the pitching moment with the lift carry on the body by wing [see Eqs. (8) and (10) here and Eqs. (9) and (11) in Ref. 1].

Acknowledgment

Support of this work by NASA Contract NAS 5-24242 to Howard University is hereby gratefully acknowledged. The authors wish to express their thanks to the Technical Officer of contract, Mr. James S. Barrowman, Code 742, at the NASA Goddard Space Flight Center in Greenbelt, Md.

References

[1] Vira, N.R. and Fan, D.N., "Closed-Form Solutions of Supersonic Wing-Body Interference," *AIAA Journal*, Vol. 20, June 1982, pp. 855-857.

[2] Pitts, W.C., Nielsen, J.N., and Kaattari, G.E., "Lift and Center of Pressure of Wing-Body-Tail Combinations at Subsonic, Transonic, and Supersonic Speeds," NASA 1307, 1959.

[3] Fan, D.N. and Vira, N.R., "Aerodynamics of Sounding Rockets," Annual Report to the NASA Goddard Space Flight Center, NASA Contract NAS5-24242, Dept. of Mechanical Engineering, Howard University, Washington, D.C., Oct. 1980.

AIAA 82-4190

Three-Dimensional Shock Structure in a Transonic Flutter Cascade

D. R. Boldman,* A. E. Buggele,† and A. J. Decker‡
NASA Lewis Research Center, Cleveland, Ohio

Introduction

THIS Note describes the results of an exploratory experiment to visualize the transonic shock structure in a linear cascade of two-dimensional airfoils which are externally oscillated in torsion. Since the flowfield contains mixed subsonic-supersonic flow, the supersonic regions can usually be observed with schlieren or shadowgraph systems.[1-2] Although certain information about the shock dynamics can be obtained from high-speed motion pictures of the schlieren images, details concerning the two-dimensionality of the shock during "simulated" flutter are obscure. The present experiment addresses this latter problem through the use of rapid double-pulse holography.[3]

Holographic interferometry has been used for the three-dimensional flow visualization of shock waves in a compressor rotor, e.g., Ref. 4. By comparing holographic and laser anemometer measurements of shock position, it could be seen that blade passage interference fringes caused by motion of the shock wave between the two exposures of a double-exposure hologram, did not always localize on the shock surface. Consequently, it is necessary to analyze and to correct for these fringe localization effects. The results in Ref. 5 indicated that one method of minimizing this fringe localization error is to establish a view of the shock which is close to the tangency at the shock surface. In principle, this condition can readily be realized by observing the flow in a two-dimensional test arrangement such as the flutter cascade used in the present investigation.

Experiment

The flow visualization experiment was performed in a cascade containing three driven biconvex airfoils as shown in Fig. 1. These two-dimensional airfoils had a thickness-to-chord ratio of 0.076, a chord of 7.62 cm, and a span of 9.65 cm. The airfoil chord-to-spacing ratio (solidity) was 1.3. The cascade stagger angle or angle between the flow direction and leading edge plane was 30 deg, typical for transonic rotor blading. Blade-to-blade similarity in shock structure was achieved through adjustable tailboards and a boundary-layer bleed system. The end wall boundary-layer thickness δ measured one chord length upstream of the cascade leading edge was approximately 1 cm.

A modified version of the mechanical drive system described in Ref. 2 was used to oscillate the airfoils. A "simulated" flutter environment was obtained by oscillating the airfoils in harmonic pitching motion about the midchord axis. In this type of motion the instantaneous angle of attack α can be expressed as

$$\alpha = \bar{\alpha}\sin\omega t + \alpha_0$$

The airfoils were driven at a nominal frequency f of 580 Hz, an amplitude $\bar{\alpha}$ of 1.2 deg, and a mean angle of attack α_0 of 6.0 deg. At the freestream Mach number M_∞ of 0.81, the reduced frequency based on the half-chord was about 0.53.

The object beam from a double-pulse ruby laser was transmitted through an optical glass window (cascade end wall) where it passed between the airfoils to the far end wall as shown in Fig. 1. There the light was diffusely reflected by means of a flat-white plastic sheet cemented to the end wall. The diffused light passed back through the airfoils and the optical glass end wall onto a high-resolution photographic plate. Two holograms, separated by a preselected delay time, were recorded on the same plate. In the reconstruction of the double image, interference fringes are formed when there is a slight difference in the refractive index fields between the two exposures. Pulse delay times of 10-20 μs yielded the best images.

Results

Initial tests were performed using the double-pass schlieren flow visualization system described in Ref. 2. The steady-state schlieren image obtained at a mean angle of attack of 6 deg and a Mach number of 0.81 is shown in Fig. 2. This figure clearly reveals a lambda-type shock near the leading edge of

Received Aug. 28, 1981; revision received Dec. 1, 1981. This paper is declared a work of the U.S. Government and therefore is in the public domain.

*Aerospace Engineer. Associate Fellow AIAA.
†Aerospace Engineer. Member AIAA.
‡Optical Physicist.

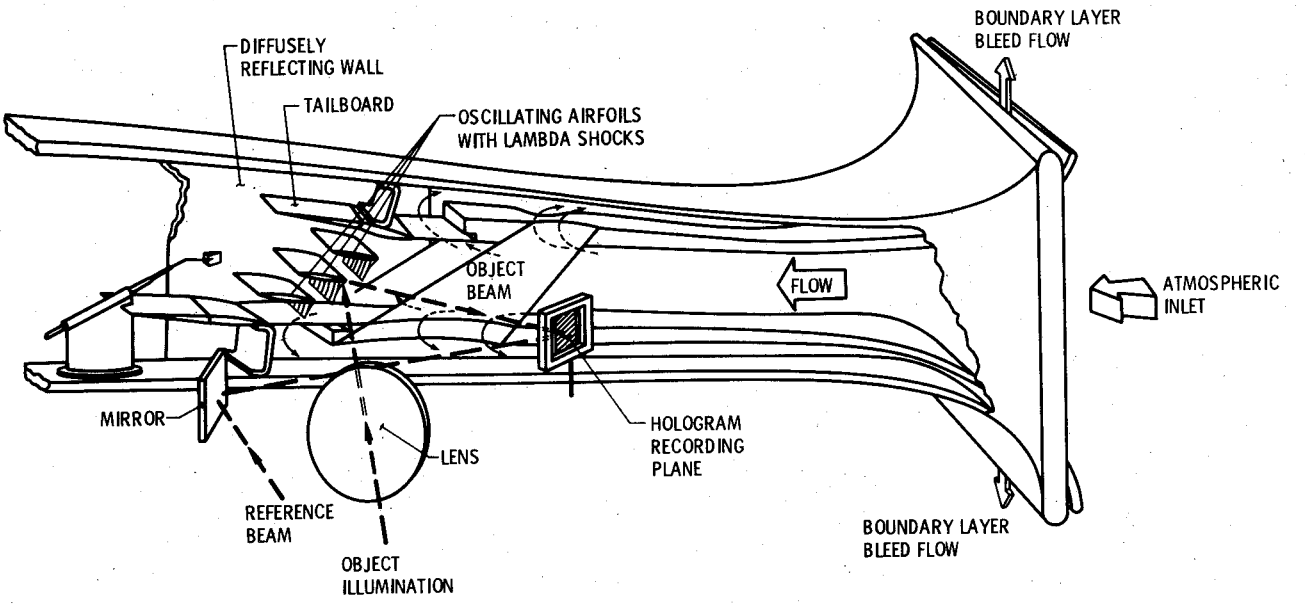

Fig. 1 Optical arrangement.

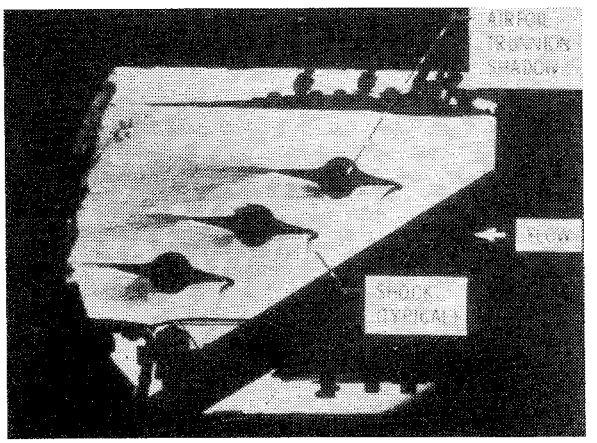

Fig. 2 Double-pass schlieren image of steady-state flow in cascade (Mach 0.81).

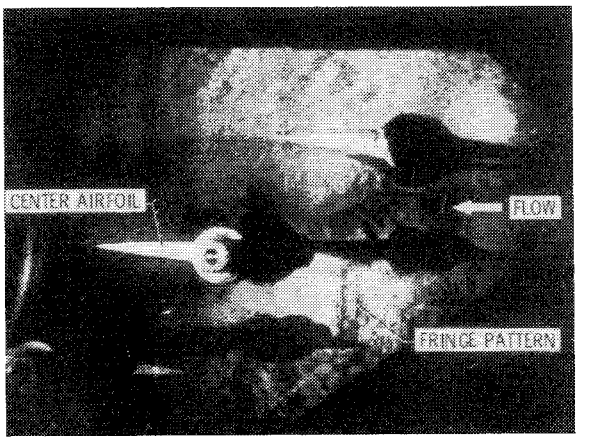

Fig. 3 Fringe pattern associated with one state of a shock wave during simulated torsional flutter ($f = 580$ Hz, Mach 0.81).

the airfoils. Subsequent high-speed motion pictures revealed that this shock persists throughout the oscillatory cycle, weakening near the minimum value of α and becoming stronger near the maximum angle of attack. The position where the shock appears most intense does not coincide with the maximum α due to a phase lag between the shock and blade motion.[2] These schlieren images are typical of the quality obtained in the double-pass optical system. An indication of the two-dimensionality of the shock surface can be obtained from images of this type on the basis of the extent or smearing of the image or possibly the appearance of multiple shocks (depending on exposure times and other factors). The shock patterns in Fig. 2 suggest that the shocks are reasonably two-dimensional at steady-state operating conditions.

An attempt was made to obtain a hologram of this same steady-state flowfield using the rapid double-exposure technique; however, because of insufficient time variations in the flow, an image of the shocks could not be obtained at the design Mach number of 0.81. Shocks were observed with stationary airfoils only during choked flow conditions ($M \approx 1.0$) in the cascade.

More than 50 holograms were obtained in the tests with oscillating airfoils. One hologram was recorded in each test by randomly triggering the laser after the airfoil oscillatory frequency became steady. In a few of the holograms a shock was not apparent. The results to be described are representative of the majority of the holograms in which a shock was observed. It is generally recognized that a single photograph of the holographic image is not as informative as an actual view of the reconstructed three-dimensional image; however, a photograph of the image viewed at a slightly oblique angle can reveal some of the three-dimensional characteristics of the shock. The following comments on shock structure are based on the results shown in Fig. 3 in conjunction with the additional information gained through visualization of the reconstructed images.

The images in Fig. 3 show that the shock on the upper airfoil is located further downstream than the shock on the center airfoil. These differences in the blade-to-blade shock patterns, which indicate a certain degree of nonperiodicity in the cascade, are consistent with the results from the schlieren imagery at steady-state conditions (Fig. 2). The shocks extend outside the field of view in the holographic images and form two-dimensional surfaces in a narrow region between the end walls as shown in Fig. 3. Analysis of the reconstructed images indicated that the width of the surface was about 33% of the passage width. This narrow but two-dimensional surface suggests an appreciable end wall shock/boundary-layer interaction, presumably due to relatively thick end wall boundary layers ($\delta \approx 1$ cm).

In many of the holographic images recorded of different states of the shock wave, there was a strong spanwise variation of the fringe pattern. Since the formation and localization of that pattern depends upon the shock slope, curvature, the positional variation in shock strength, and the time variation of these quantities, there is some evidence of a spanwise variation in the space- and time-dependent properties of the shock wave.

Conclusions

The results, based on observations of holographic images, reveal a relatively narrow two-dimensional shock surface moving over airfoils which are driven to simulate transonic torsional flutter. However, some of these same holograms revealed a spanwise variation in the shock properties. This latter behavior warrants further investigation for it could have important ramifications concerning the use of experimental results from driven transonic cascades of this type. This exploratory study also indicates the feasibility of using diffuse-illumination, rapid double-exposure holographic interferometry for visualization of the shock structure in a transonic flutter cascade.

References

[1] Riffel, R. E. and Rothrock, M. D., "Experimental Determination of Unsteady Blade Element Aerodynamics in Cascades, Vol. 1: Torsion Mode Cascade Final Report," Detroit Diesel Allison Div., General Motors Corp., Indianapolis, Ind., Rept. EDR-10119-VOL-1, June 1980 (also NASA CR-159831).

[2] Boldman, D. R. and Buggele, A. E., "Wind Tunnel Tests of a Blade Subjected to Midchord Torsional Oscillation at High Subsonic Stall Flutter Conditions," NASA TM-78998, 1978.

[3] Wuerker, R. F., Kobayashi, R. J., Heflinger, L. O., and Ware, T. C., "Application of Holography to Flow Visualization Within Rotating Compressor Blade Row," AiResearch Mfg. Co., Los Angles, Rept. AIRESEARCH-73-9489, Feb. 1974 (also NASA CR-121264).

[4] Strazisar, A. J. and Chima, R. V., "Comparison Between Optical Measurements and a Numerical Solution of the Flow Field in a Transonic Axial-Flow Compressor Rotor," AIAA Paper 80-1078, June 1980.

[5] Decker, A. J., "Holographic Flow Visualization of Time-Varying Shock Waves," *Applied Optics*, Vol. 20, No. 18, Sept. 1981, pp. 3120-3127.

AIAA 82-4191

"Coriolis Resonance" within a Rotating Duct

M. Kurosaka* and J. E. Caruthers†
University of Tennessee Space Institute, Tullahoma, Tenn.

CURIOUSLY enough, although investigations[1] on unsteady disturbances in axial flow compressors abound, little appears to be available in the open literature for centrifugal machines. However, the flow-induced vibration problems in centrifugal compressors are no less frequent or harassing than their axial-flow counterparts.

In contrast to the axial-flow compressors, in the radial-flow machines we expect the Coriolis force to exert dominating effects upon the unsteady disturbances. For one thing, the Coriolis force more closely couples the disturbances in two flow directions: the radial and circumferential directions. For another—and more important—when we recall that a) the Coriolis force is proportional to twice the shaft-rotation frequency (2Ω) and b) the time-derivative terms of the equation of motion are proportional to the frequency of flow disturbances (ω), there looms an intriguing possibility that a resonance might occur at $\omega=2\Omega$. To the extent that the aforementioned dynamic coupling in two flow directions exists, such a resonance would be akin to the one in the mechanical vibration of a two-degree-of-freedom system. Aside from this, from the aeroacoustic point of view, the pronounced effect of rotation may alter markedly the cut-off condition.

To explore these questions and to do so without being entangled in encumbering analysis, we pose a simple, model problem: an investigation into unsteady disturbances with frequency ω within a radial duct, which rotates with angular speed Ω about the z axis (Fig. 1). In the absence of unsteady disturbances, the steady velocity u_0 is directed toward the radial direction; the height of the duct in the z direction is uniform.

We assume that the flow is compressible, inviscid and the fluid is a perfect gas. We take the coordinate system fixed to the rotating duct and separate the unsteady part, denoted by primes, from the base, steady part with subscript *0*

$$u_r=u_0+u', \quad u_\theta=v', \quad u_z=w'$$

$$p=p_0+p', \quad \rho=\rho_0+\rho', \quad s=s_0+s' \tag{1}$$

where s is the entropy, the other notation being standard. By substituting Eq. (1) into the governing equations, written in cylindrical coordinates, and neglecting the second-order terms in disturbances, we obtain, as usual, two sets of equations: one for the steady part and the other for unsteady disturbances, the latter being of our central interest.

We further assume the following: 1) the wavelength of the unsteady disturbances in the radial direction is small compared to the radial length of the duct; 2) u_0 does not vary in the θ and z directions; 3) p_0, ρ_0, and a_0 (acoustic speed) do not vary in the z direction; 4) $2\Omega r\Theta/u_0 \ll 1$, when Θ shown in Fig. 1 is the half-angle of the duct; and 5) s_0 is a constant. On the assumption of point 4 the derivatives of the steady parts in the radial direction are small compared to the variation of the unsteady disturbances in the same direction; for example,

$$\frac{\partial p_0}{\partial r} \ll \frac{\partial p'}{\partial r}$$

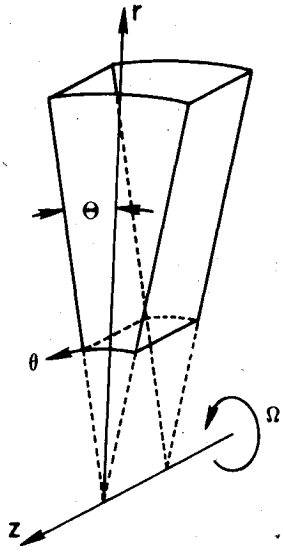

Fig. 1 Radially divergent rotating duct.

Received Sept. 4, 1981; revision received Dec. 11, 1981.

*Professor of Aerospace and Mechanical Engineering. Associate Fellow AIAA.

†Associate Professor of Engineering Science and Mechanics.